



King's Research Portal

DOI:

[10.1016/j.crad.2018.08.012](https://doi.org/10.1016/j.crad.2018.08.012)

Document Version

Peer reviewed version

[Link to publication record in King's Research Portal](#)

Citation for published version (APA):

Gibbs, T., Villa, A. D. M., Sammut, E., Jeyabraba, S., Carr-White, G., Ismail, T. F., Mullen, G., Ganeshan, B., & Chiribiri, A. (2018). Quantitative assessment of myocardial scar heterogeneity using cardiovascular magnetic resonance texture analysis to risk stratify patients post-myocardial infarction. *Clinical Radiology*. <https://doi.org/10.1016/j.crad.2018.08.012>

Citing this paper

Please note that where the full-text provided on King's Research Portal is the Author Accepted Manuscript or Post-Print version this may differ from the final Published version. If citing, it is advised that you check and use the publisher's definitive version for pagination, volume/issue, and date of publication details. And where the final published version is provided on the Research Portal, if citing you are again advised to check the publisher's website for any subsequent corrections.

General rights

Copyright and moral rights for the publications made accessible in the Research Portal are retained by the authors and/or other copyright owners and it is a condition of accessing publications that users recognize and abide by the legal requirements associated with these rights.

- Users may download and print one copy of any publication from the Research Portal for the purpose of private study or research.
- You may not further distribute the material or use it for any profit-making activity or commercial gain
- You may freely distribute the URL identifying the publication in the Research Portal

Take down policy

If you believe that this document breaches copyright please contact librarypure@kcl.ac.uk providing details, and we will remove access to the work immediately and investigate your claim.

Background

In recent years, advances in the management of myocardial infarction (MI) have led to significant improvements in patient survival. However, though patients overcome the index event, many are left with impaired left ventricular function and carry a risk of life-threatening arrhythmia secondary to impaired left ventricle (LV) function and the presence of myocardial scar. The occurrence of ventricular arrhythmia can result in cardiac arrest and sudden cardiac death (SCD)¹. Recent guidance recommends implantable cardioverter defibrillator (ICD) implantation for patients deemed at high risk for such events. Currently, ICD is recommended for patients after MI in the presence of significant LV dysfunction^{1,2}. However, arrhythmias and SCD are also seen in patients with preserved LV ejection fraction (EF) and the incidence of appropriate shocks in patients receiving an ICD on the basis of current guidelines is low³. Therefore, there remains significant debate about how to best identify high-risk patients and avoid the implantation of unnecessary devices. Many patients now routinely undergo cardiac magnetic resonance (CMR) with late gadolinium enhancement (LGE) as part of their evaluation. This test is considered the reference standard for the identification of myocardial scar and fibrosis, and for the quantification of LVEF. Previous data demonstrate that even small areas of scar, which do not impact on LVEF, can result in arrhythmic events and it has previously been suggested that scar could be a sensitive marker of increased arrhythmic risk^{4–6}. On a histopathological level, scar is complex and previous studies using contrast-enhanced CMR delineated two distinct patterns: (1) the scar core, made up of fibrous tissue, characterised by higher signal intensity on LGE images; and (2) heterogeneous tissue, containing necrotic tissue interspersed with bundles of viable myocytes, associated with lower signal intensity compared

with the core of the scar ⁷. It has been suggested that slow local conduction through these heterogeneous regions of scar could be responsible for development of lethal re-entrant arrhythmias ^{8,9}. Recent studies performed with the aid of numerical simulations have shown that the spatial heterogeneity of fibrosis correlates directly with the risk of arrhythmia and that this is more pronounced with the increase of both the spatial size and the degree of heterogeneity ¹⁰.

Quantitative texture analysis (TA) is a tool previously described for the assessment and stratification of solid tumours ^{11,12}. To the best of our knowledge, TA has not previously been applied to the analysis of CMR images, if we exclude some preliminary work [REDACTED] ¹³. CMR-TA has the potential to be applied to the analysis of LGE images, providing additional information on scar heterogeneity ¹³. One such TA technique is the filtration-histogram approach where the filtration step extracts and enhances features or objects of different sizes, allowing quantification using histogram-based statistical parameters, which evaluate the grey-level pixel distribution. This filtration-histogram technique has been shown to describe the different components of macroscopic heterogeneity ¹¹. This is done in terms of standard descriptors such as mean, standard deviation, skewness and kurtosis ^{12,14}. The aim of this exploratory study was to apply quantitative CMR-TA to the assessment of LGE images in patients with previous MI and to determine whether texture analysis-derived indices may provide insights to facilitate better risk stratification in this cohort.

Materials and Methods

Patient population

Patients referred on clinical grounds for CMR assessment of myocardial viability were retrospectively identified using electronic hospital records. The study population consisted of consecutive patients who had undergone CMR, with evidence of sub-endocardial or transmural ischaemic scar on LGE imaging. Patients with suspected infiltrative cardiomyopathy (including cardiac haemochromatosis, amyloidosis or sarcoidosis), myocarditis, or non-ischaemic cardiomyopathies, such as hypertrophic cardiomyopathy or dilated cardiomyopathy, were excluded. In order to exclude histologically evolving scar, patients with a recent (<60 days) history of acute coronary syndrome were also excluded. All patients gave written consent to the CMR scan. Local research ethics committee approval was granted (REC 15/NS/003) for retrospective analysis of the data.

CMR imaging protocol

CMR imaging was performed using standardised acquisition protocols using a 1.5-T CMR system with a 32-channel cardiac phased array surface coil (Philips Healthcare, Best, The Netherlands)¹⁵. The standard clinical CMR study consisted of a stack of breath-hold short axis cine steady-state free precession slices covering the LV (slice thickness 8mm, in plane spatial resolution 448x448). These were acquired for quantification of left ventricular (LV) volumes, function and mass according to standardised post-processing methods¹⁶. An inversion-recovery gradient-echo pulse sequence for LGE assessment was used to acquire a stack of short axis slices 15-20 minutes after contrast injection (Gadobutrol, Bayer-Schering Pharma, Berlin, Germany,

0.2mmol/kg body weight). Typical acquisition parameters for LGE imaging were TR/TE/turbo gradient factor of 3.5ms/2.0ms/25, enabling a temporal resolution of 88 ms.

LGE images were used to identify and measure the extent of ischaemic scar (percentage of total LV mass) and for texture analysis post-processing. To this purpose, a commercially available software package was used (CMR42, v5.6.4, Circle Cardiovascular Imaging, Calgary, Canada).

CMR texture analysis – CMR-TA

CMR-TA was performed on LGE images selected at basal, mid-ventricular and apical level according to standard anatomical positions¹⁵. Areas of scar at each level were manually segmented and then analysed using TexRAD research software (TexRAD Ltd., www.texrad.com, Feedback Plc, Cambridge, UK). In brief, a region of interest (ROI) was drawn around areas of enhancement ensuring that the scar border but no surrounding tissue was included. The ROI therefore encompassed the scar core and the heterogenous region. If there were multiple scars in a short axis slice, values were averaged together. Manual segmentation of scar core and heterogenous region was performed with the consensus of two expert CMR readers blinded to patient identifiers and clinical data.

Images were then filtered using a Laplacian of Gaussian band-pass (similar to a non-orthogonal Wavelet approach) filtration step to extract and enhance features of different sizes based on the spatial scale filter (SSF) values varying from 2-6mm in radius (where 2mm corresponds to fine texture features, 3-5mm corresponds to medium texture features and 6mm corresponds to coarse texture features; [Figure 1](#)). Following image filtration, histogram analysis of pixel intensity was performed to quantify each filtered image texture map in terms of statistical

parameters such as mean, standard deviation, entropy, skewness and kurtosis. With this filtration approach, the Gaussian part of the filter reduces the impact of noise component and the Laplacian part enhances subtle features (biologically relevant "heterogeneity") quantifiable by the histogram analysis. These features are potentially relevant for disease diagnosis and prognostic assessment and are not visible to the naked eye on conventional (unfiltered) images. A detailed description of the filtration-histogram technique can be found in the literature ¹². Skewness is a statistical term that describes the asymmetry of a data set from the normal distribution. A negative skewness is where the data points are skewed to the right of a normal bell-shaped curve, whereas a positive skewness involves a leftward skew of the data points. Meanwhile kurtosis quantifies the sharpness of the peak of a frequency-distribution curve. A positive kurtosis indicates a more peaked histogram than a normal distribution, whilst a data-set that is flatter than a normal distribution correlates with a negative kurtosis (Figure 2). In this study, average, maximum and minimum skewness and kurtosis were measured in each patient.

Outcome measures and follow up

Patients were followed up from the point of their initial CMR scan. The primary end-point was a composite of ventricular fibrillation (VF), sustained ventricular tachycardia (VT) (defined as ventricular tachycardia with a rate $>120 \text{ min}^{-1}$ lasting longer than 30 seconds) with haemodynamic compromise and/or requiring cardioversion, appropriate ICD discharge or unexplained syncope.

Statistical analysis

Continuous variables are expressed as mean \pm standard deviation (SD), or as median and interquartile range (IQR) in cases where the data were not normally distributed. Categorical data are summarised as frequencies and percentages. The Student's *t* test was used to compare mean values of continuous data between the group of patients who suffered events and those who did not. Where the data was non-normally distributed, the Mann-Whitney U test was used for group-wise comparison. The relationship of the various imaging and clinical markers with patient survival were assessed using Kaplan-Meier (KM) survival analysis. Only characteristics significantly different between the two groups at the Student's *t* test or Mann-Whitney test were included in the univariable analysis. This was undertaken to minimise the issue of multiple statistical testing and reduce the false discovery rates resulting from multiple testing. Optimal thresholds for the above identified texture parameters were determined using Receiver Operating Characteristics (ROC) analysis and employed for KM analysis. The log-rank test was employed to assess the difference between the survival distributions. In case of the other clinical and imaging parameters, previously validated thresholds were employed for the KM analysis. KM curves for patients above and below each threshold were constructed to display the proportion of patients surviving at a given time. We evaluated the survival probability according to the factors significant on univariable analysis using the Cox proportional hazards model. Multivariable analysis was used to adjust for potential confounding. The intra- and inter-observer reproducibility of TA was quantified using the intraclass coefficient of correlation.

All data were analysed using Microsoft Excel and IBM SPSS Statistics version 22 for Macintosh, with two-tailed values of $p < 0.05$ considered significant.

126

127 **Results**

128 The study cohort consisted of 76 patients with a median period of follow up of 371.5 days (IQR
129 135-645 days). During follow up, eight patients (10.5%) developed VT, two patients (2.6%)
130 suffered at least one episode of VF and five patients (6.6%) experienced syncopal events
131 suspected to relate to ventricular arrhythmias, leading to ICD implantation. This comprised a
132 total of 14 patients (18%) with events at follow up. Baseline characteristics of patients are
133 summarised in [Table 1](#). The mean age of patients was 61.5±11.4 years, 80% were male, 60%
134 had undergone prior revascularisation and the mean LVEF was 50% (±10%). Five patients had
135 ICD implantation during follow-up and all of these patients were within the events group.

136

137 ***Predictors of adverse events***

138 *Baseline characteristics*

139 Patient characteristics related to the primary endpoint are listed in [Table 1](#). There was no
140 significant difference in gender or clinical variables between those who suffered events
141 compared to those who did not, though patients in the event group were significantly older.
142 Furthermore, patients who suffered ventricular arrhythmic events or unexplained syncope
143 following MI had an on average higher LV end-diastolic volume (EDV), higher end-systolic
144 volume (ESV), larger left atrium (LA) and lower left ventricular ejection fraction (LVEF). Notably,
145 there was no relationship between the total scar burden and occurrence of events.

CMR-TA to assess scar heterogeneity

The median amount of tissue analysed was 2.9g of tissue (IQR, 2.0g to 4.3g) in the events group and 2.7g (IQR, 1.9g to 4.5g) in the group that did not suffer events ($p=0.61$).

Table 2 represents the means \pm SD for all the texture parameters employed in the study and their relationship to events on univariable analysis. Patients who had an event had a higher average and maximum kurtosis ($kurtosis_{avg}$ and $kurtosis_{max}$), a trend seen across all filter levels but only statistically significant in the coarser filter scales, SSF=5 ($p=0.007$ and 0.005 respectively) and SSF=6 ($p=0.015$ and 0.025 respectively). Minimum skewness ($skewness_{min}$) at fine filter scale (SSF=2) was found to be significantly lower in the events group ($p=0.046$).

Survival analysis

Figure 3 shows KM survival plots based on previously validated thresholds and testing the association between clinical factors and prognosis¹⁷. Age (>65 years, $p=0.03$), LVEF ($<35\%$, $p=0.048$) and indexed LVEDV (>86 ml/m², $p=0.006$) stratified patients for events. LA area (>24 cm²) was the only factor, amongst those tested, not statistically associated with a higher event rate ($p=0.27$).

Table 3 and Figure 4 demonstrate the results from KM analysis only using the texture parameters highlighted above, which significantly differentiated between patients' groups. Specifically, a higher $kurtosis_{max}$ and $kurtosis_{avg}$ value at coarse texture scale (SSF=5 and SSF=6) and lower $skewness_{min}$ value at fine texture scale (SSF=2) predicted poor survival (Table 3).

165 Interestingly, none of the patients reclassified by TA as low risk had any events, with the
166 exception of one patient in the analysis by kurtosis_{avg} at SSF=5. This was not the case for other
167 significant imaging and clinical markers of survival (e.g. age, LVEF, LA area and LVEDV), where
168 several events occurred in both groups.

169 ***Predictors of survival***

170 The Cox model was used to identify factors involved in prediction of survival. When the Cox
171 model including TA parameters significant on univariate analysis were tested and corrected for
172 confounders such as age and LVEF, kurtosis_{avg} at SSF=5 TA and LVEF retained significant
173 independent association with events (p=0.007 and p=0.006, respectively), whereas age and
174 other TA parameters were no longer significant.

175 ***Reproducibility analysis***

176 Reproducibly analysis was performed on TA parameters which were associated with events at
177 univariate analysis. Intra-observer reproducibility was excellent for skewness SSF=2 (r=0.96),
178 kurtosis SSF=5 (r=0.99) and kurtosis SSF=6 (r=0.99). Inter-observer reproducibility was good for
179 skewness SSF=2 (r=0.98). Good inter-observer reproducibility was measured for kurtosis SSF=5
180 (r=0.84) and kurtosis SSF=6 (r=0.89).

181 ***ROC analysis***

182 ROC curves for texture analysis and standard parameters to the paper are summarised in [Table](#)
183 [4](#). ROC curves for kurtosis_{avg} SSF=5 and LVEF are demonstrated in [Figure 5](#).

184

Discussion

Myocardial scar heterogeneity as assessed by CMR-TA is associated with arrhythmic events in patients with previous MI. In particular, a higher kurtosis value at coarse texture scale and lower skewness value at fine texture scale were associated with an adverse outcome. These findings echo the results of previous preliminary work using TA [REDACTED] on patients with existing ICDs, which also demonstrated in a different and smaller group of patients that higher kurtosis with application of a coarse filter and lower skewness with application of a fine filter was able to predict post-MI VT or VF¹³. Interestingly, our data did not show any significant difference in overall scar burden between the event and non-event groups. This possibly suggests that scar heterogeneity assessed by TA could provide independent and complementary information to scar burden, although this hypothesis will have to be tested in future prospective outcome studies. Moreover, our data confirmed the association between increased age, reduced LVEF, and increased indexed LV EDV with the development of post-MI arrhythmias.

Substantial advances in acute management of myocardial infarction have led to significant improvements in patient survival. Large numbers of these patients are however left with impairment of LV function due to myocardial scarring and an increased risk of life-threatening ventricular arrhythmias. Current guidelines focus on LVEF as the key determinant of the need for ICD therapy; however, only the minority of patients who undergo implantation on this basis receive appropriate ICD therapies and, on the other hand, some patients with normal LV

205 function present with arrhythmias or SCD ³. This has led to significant efforts to refine
206 biomarkers to guide appropriate risk stratification and ICD implantation.

207 Myocardial scar in patients with previous MI is accepted as a source of ventricular arrhythmias
208 ^{9,18}. Previous data demonstrated that even small areas of scar, which do not impact on LVEF,
209 can result in arrhythmic events ^{4,5}. Bello *et al* ¹⁹ was the first to directly analyse the relationship
210 between some morphological features of myocardial scar and the induction of ventricular
211 arrhythmia. Scar surface and mass, as characterised by CMR, were shown to be better
212 predictors of inducible monomorphic VT than LVEF ¹⁹. This study however did not provide any
213 insight on the role of scar heterogeneity.

214 Electrical mapping studies have shown that the border areas of infarcted myocardial tissue,
215 found adjacent to dense scar, are responsible for this arrhythmogenicity ^{7,9,20}. This area, also
216 known as grey zone, is a heterogeneous region composed of isolated bundles of viable
217 myocytes interwoven with fibrous tissue ²¹. Grey zone regions conduct electrical activity more
218 slowly than the surrounding myocardium, leading to the development of re-entrant VT ^{9,22,23}.

219 Subsequent studies have shown that more extensive grey zone at the periphery of a scar
220 strongly correlates with greater VT inducibility, and that the extent of grey zone provides
221 incremental prognostic value beyond LVEF ²⁴. More recently the same findings have been made
222 in spontaneous VT following myocardial infarction ²⁵. These studies provide powerful evidence
223 that factors, other than the presence and extent of scar, play a pivotal role in the pathogenesis
224 of ventricular arrhythmias.

225 The current study is the first to go beyond the assessment of the extent of the grey zone and to
226 consider the make-up of the heterogeneous infarct area itself, testing the hypothesis that scar
227 complexity is linked to the development of arrhythmias. TA was initially developed in the field
228 of oncology, where the complexity of solid tumour tissue has been shown to predict prognosis,
229 assess disease severity and treatment response evaluation ¹¹. Our study demonstrates for the
230 first time *in vivo* that specific features of the texture of the scar are linked to arrhythmogenicity.
231 The same features have previously been associated with increased risk of arrhythmic events in
232 pathologic and computational modelling studies ¹⁰. Our findings are keeping with current
233 understanding of the pathophysiological mechanisms linking the presence of scar to the onset
234 of re-entrant arrhythmias.

235 For the interpretation of the biological meaning of the observed values of skewness and
236 kurtosis, we can refer to previously published literature ¹². Higher kurtosis value indicates
237 increased visual contrast (intensity variation) in the objects highlighted by filtration in relation
238 to the background tissue. A lower skewness value indicates the presence of darker areas. In
239 combination, these features suggest a more heterogeneous scar, comprising areas of grey zone
240 interspersed with areas of denser scar. Interestingly, there was no significant difference
241 between the two groups in terms of scar burden, probably indicating that these texture
242 features of scar heterogeneity could provide independent information from the presence or
243 absence and the burden of scar.

244 Our findings are in keeping with recent data investigating the role of scar heterogeneity in the
245 genesis of arrhythmia by means of mathematical models. This study assessed the role of mean

fibrosis level and of the extent and spatial size of the heterogeneity and demonstrated that a more heterogeneous distribution of fibrosis was associated with an increased likelihood of arrhythmias and that the main mechanism of this dependency was the presence of localised tissue patches with more severe degrees of fibrosis ¹⁰.

LGE images were acquired in this study according to standard clinical practice and SCMR guidelines, with a relatively short acquisition time in order to limit the amount of motion ¹⁵. This is a particularly important aspect as motion could potentially result in the inclusion of blood-pool in the region of interest, particularly when small subendocardial scars are analysed, or might contribute to a loss of information when finer texture is analysed. A significant improvement on this side will be allowed by the advent of a new generation of sequences for “dark-blood” LGE which may further improve scar conspicuity ^{26,27}.

Study limitations

This is a pilot study to assess the potential for TA to be used as an added marker of risk and estimate the effect size in view of future adequately powered studies to test an independent association between scar texture features and events. Our results suggest excellent predictivity for events using TA parameters. However, optimised cut off values were used based on ROC analysis as this was a pilot exploratory study, whereas cut off values from the literature were used for the evaluation of standard markers of risk, likely resulting in a relative underestimation of the predictivity of the latter. We have included multivariable Cox regression analysis and have demonstrated the presence of an independent association between TA (kurtosis SSF=5 average) and events. Given the pilot nature of this study and the relatively limited sample size,

267 these findings will need to be confirmed by a future prospective study on a larger population of
268 patients.

269 **Conclusion**

270 The use of texture analysis in addition to standard clinical and functional data derived from
271 CMR such as the presence of scar and LVEF (e.g. a multi-parametric approach) may provide
272 additional information to guide risk stratification of patients post myocardial infarction.

273

274 **Abbreviations**

275 Myocardial infarction (MI); Sudden cardiac death (SCD); Left ventricular ejection fraction (LVEF);
276 Late gadolinium enhancement (LGE); Cardiac magnetic resonance (CMR); Implantable cardiac
277 defibrillators (ICDs); Left ventricle (LV); Region of interest (ROI); Spatial scale filter (SSF);
278 Ventricular tachycardia (VT); Ventricular fibrillation (VF); End-diastolic volume (EDV); End-
279 systolic volume (ESV); Left atrium (LA); Left ventricular ejection fraction (LVEF); New York Heart
280 Association (NYHA); Texture analysis (TA).

281

282 **Declarations**

283 ***Ethics approval and consent to participate***

284 Local research ethics committee approval was granted (REC 15/NS/003) for retrospective
285 enrolment of patients and analysis of the imaging and clinical data. All patients gave written
286 consent to the CMR scan.

287 ***Consent for publication***

288

289 Not applicable.

290

291

292 ***Availability of data and material***

293

Anonymized datasets used and/or analyzed during the current study are available from the
corresponding author on reasonable request.

Competing interests

[REDACTED]

[REDACTED]

[REDACTED]

[REDACTED]

[REDACTED]

313 **References**

- 314 1 Moss AJ, Zareba W, Hall WJ, *et al.* Prophylactic implantation of a defibrillator in patients with
315 myocardial infarction and reduced ejection fraction. *N Engl J Med* 2002; **346**: 877–83.
- 316 2 Bardy GH, Lee KL, Mark DB, *et al.* Amiodarone or an implantable cardioverter-defibrillator for
317 congestive heart failure. *N Engl J Med* 2005; **352**: 225–37.
- 318 3 Buxton AE. Identifying the high risk patient with coronary artery disease--is ejection fraction all you
319 need? *J Cardiovasc Electrophysiol* 2005; **16 Suppl 1**: S25–27.
- 320 4 Kwong RY, Chan AK, Brown KA, *et al.* Impact of unrecognized myocardial scar detected by cardiac
321 magnetic resonance imaging on event-free survival in patients presenting with signs or symptoms of
322 coronary artery disease. *Circulation* 2006; **113**: 2733–43.
- 323 5 Kwong RY, Sattar H, Wu H, *et al.* Incidence and prognostic implication of unrecognized myocardial
324 scar characterized by cardiac magnetic resonance in diabetic patients without clinical evidence of
325 myocardial infarction. *Circulation* 2008; **118**: 1011–20.
- 326 6 Chen Z, Sohal M, Voigt T, *et al.* Myocardial tissue characterization by cardiac magnetic resonance
327 imaging using T1 mapping predicts ventricular arrhythmia in ischemic and non-ischemic
328 cardiomyopathy patients with implantable cardioverter-defibrillators. *Heart Rhythm* 2015; **12**: 792–
329 801.
- 330 7 Schmidt A, Azevedo CF, Cheng A, *et al.* Infarct tissue heterogeneity by magnetic resonance imaging
331 identifies enhanced cardiac arrhythmia susceptibility in patients with left ventricular dysfunction.
332 *Circulation* 2007; **115**: 2006–14.
- 333 8 Verma A, Marrouche NF, Schweikert RA, *et al.* Relationship between successful ablation sites and the
334 scar border zone defined by substrate mapping for ventricular tachycardia post-myocardial infarction. *J*
335 *Cardiovasc Electrophysiol* 2005; **16**: 465–71.
- 336 9 de Bakker JM, van Capelle FJ, Janse MJ, *et al.* Reentry as a cause of ventricular tachycardia in patients
337 with chronic ischemic heart disease: electrophysiologic and anatomic correlation. *Circulation* 1988;
338 **77**: 589–606.
- 339 10 Kazbanov IV, ten Tusscher KHWJ, Panfilov AV. Effects of Heterogeneous Diffuse Fibrosis on
340 Arrhythmia Dynamics and Mechanism. *Sci Rep* 2016; **6**. DOI:10.1038/srep20835.
- 341 11 Davnall F, Yip CSP, Ljungqvist G, *et al.* Assessment of tumor heterogeneity: an emerging imaging
342 tool for clinical practice? *Insights Imaging* 2012; **3**: 573–89.
- 343 12 Miles KA, Ganeshan B, Hayball MP. CT texture analysis using the filtration-histogram method: what
344 do the measurements mean? *Cancer Imaging Off Publ Int Cancer Imaging Soc* 2013; **13**: 400–6.
- 345 13 Ali N, Mullen G, Chiribiri A. Risk stratification of post-MI patients for ICD implantation using texture
346 analysis to quantify heterogeneity of scar. *J Cardiovasc Magn Reson* 2015; **17**: Q14.
- 347 14 Ganeshan B, Miles KA. Quantifying tumour heterogeneity with CT. *Cancer Imaging Off Publ Int*
348 *Cancer Imaging Soc* 2013; **13**: 140–9.

- 349 15 Kramer CM, Barkhausen J, Flamm SD, Kim RJ, Nagel E, Society for Cardiovascular Magnetic
350 Resonance Board of Trustees Task Force on Standardized Protocols. Standardized cardiovascular
351 magnetic resonance (CMR) protocols 2013 update. *J Cardiovasc Magn Reson Off J Soc Cardiovasc*
352 *Magn Reson* 2013; **15**: 91.
- 353 16 Schulz-Menger J, Bluemke DA, Bremerich J, *et al.* Standardized image interpretation and post
354 processing in cardiovascular magnetic resonance: Society for Cardiovascular Magnetic Resonance
355 (SCMR) board of trustees task force on standardized post processing. *J Cardiovasc Magn Reson Off J*
356 *Soc Cardiovasc Magn Reson* 2013; **15**: 35.
- 357 17 Hudsmith LE, Petersen SE, Francis JM, Robson MD, Neubauer S. Normal human left and right
358 ventricular and left atrial dimensions using steady state free precession magnetic resonance imaging. *J*
359 *Cardiovasc Magn Reson Off J Soc Cardiovasc Magn Reson* 2005; **7**: 775–82.
- 360 18 Richards DA, Blake GJ, Spear JF, Moore EN. Electrophysiologic substrate for ventricular tachycardia:
361 correlation of properties in vivo and in vitro. *Circulation* 1984; **69**: 369–81.
- 362 19 Bello D, Fieno DS, Kim RJ, *et al.* Infarct morphology identifies patients with substrate for sustained
363 ventricular tachycardia. *J Am Coll Cardiol* 2005; **45**: 1104–8.
- 364 20 Horowitz LN, Harken AH, Kastor JA, Josephson ME. Ventricular resection guided by epicardial and
365 endocardial mapping for treatment of recurrent ventricular tachycardia. *N Engl J Med* 1980; **302**: 589–
366 93.
- 367 21 Chen Z, Sohal M, Voigt T, *et al.* Myocardial tissue characterization by cardiac magnetic resonance
368 imaging using T1 mapping predicts ventricular arrhythmia in ischemic and non-ischemic
369 cardiomyopathy patients with implantable cardioverter-defibrillators. *Heart Rhythm Off J Heart*
370 *Rhythm Soc* 2015; **12**: 792–801.
- 371 22 Ursell PC, Gardner PI, Albala A, Fenoglio JJ, Wit AL. Structural and electrophysiological changes in
372 the epicardial border zone of canine myocardial infarcts during infarct healing. *Circ Res* 1985; **56**:
373 436–51.
- 374 23 Dillon SM, Allessie MA, Ursell PC, Wit AL. Influences of anisotropic tissue structure on reentrant
375 circuits in the epicardial border zone of subacute canine infarcts. *Circ Res* 1988; **63**: 182–206.
- 376 24 Yan AT, Shayne AJ, Brown KA, *et al.* Characterization of the peri-infarct zone by contrast-enhanced
377 cardiac magnetic resonance imaging is a powerful predictor of post-myocardial infarction mortality.
378 *Circulation* 2006; **114**: 32–9.
- 379 25 Roes SD, Borleffs CJW, van der Geest RJ, *et al.* Infarct tissue heterogeneity assessed with contrast-
380 enhanced MRI predicts spontaneous ventricular arrhythmia in patients with ischemic cardiomyopathy
381 and implantable cardioverter-defibrillator. *Circ Cardiovasc Imaging* 2009; **2**: 183–90.
- 382 26 Holtackers RJ, Chiribiri A, Schneider T, Higgins DM, Botnar RM. Dark-blood late gadolinium
383 enhancement without additional magnetization preparation. *J Cardiovasc Magn Reson Off J Soc*
384 *Cardiovasc Magn Reson* 2017; **19**: 64.
- 385 27 Peel SA, Morton G, Chiribiri A, Schuster A, Nagel E, Botnar RM. Dual inversion-recovery mr
386 imaging sequence for reduced blood signal on late gadolinium-enhanced images of myocardial scar.
387 *Radiology* 2012; **264**: 242–9.

388

389

Figure and Table Legends

Figure 1: Texture analysis filtration technique. Late gadolinium enhanced cardiac magnetic resonance image with the myocardial scar and corresponding images selectively displaying fine (spatial scaled filter (SSF) 2), medium (SSF4) and coarse (SSF5) lesion texture respectively. These varying textures correspond to myocardial scar features of different sizes and intensity variations extracted by the image filter.

Figure 2:

A: Graphs demonstrating a negative and positive skewed histogram. Skewness is a measure of the asymmetry of a distribution. The skewness value can be positive or negative. Negative skew indicated that the tail on the left side of the histogram is longer or fatter than the right side. Positive skew indicates that the tail is longer or fatter on the right side than the left side. A zero value occurs when the tails either side of the mean balance out, indicating an even distribution.

B: An illustration of positive and negative kurtosis compared to a normal distribution. Kurtosis is a measure of the peakedness of a distribution. The kurtosis value can be positive or negative. In comparison to a normal (Gaussian) distribution, a positive kurtosis indicates a more peaked histogram. A negative kurtosis correlates with a flatter histogram than that of a Gaussian distribution.

Figure 3: Kaplan-Meier analysis of standard parameters of arrhythmic risk. The difference in event-free survival when patients are stratified according to previously validated thresholds for age, LA size, LVEDV/m² and LVEF are demonstrated. LVEF = left ventricular ejection fraction; EDV = end-diastolic volume; LA = left atrium

Figure 4: Kaplan-Meier survival analysis of texture analysis parameters. Kaplan-Meier curves demonstrate the difference in event-free survival when patients are stratified according to average kurtosis when SSF5 (A) and SSF6 (B) filter levels are applied; maximum kurtosis when SSF5 (C) and SSF6

are applied; and minimum skewness when SSF2 (E) is applied. The thresholds used to stratify patients are optimised cut-offs from ROC analysis.

SSF = spatial scale filter.

[Figure 5: Receiver operating characteristic curves for kurtosis SSF5 average and left ventricular ejection fraction \(LVEF\).](#)

[Table 1: Demographics and baseline CMR characteristics.](#) Values are mean plus or minus standard deviation, median and interquartile range or n (%). p Value pertains to the comparison between groups with and without ventricular arrhythmia/unexplained syncope events. CABG= coronary artery by-pass graft, PCI= percutaneous coronary intervention, MRI= magnetic resonance imaging, LVEF = left ventricular ejection fraction; EDV = end-diastolic volume; ESV = end-systolic volume; RVEF = right ventricular ejection fraction; LA = left atrium; RA = right atrium.

[Table 2: Detailed results of TA-CMR for SSF of 2 to 6.](#) Values are mean plus or minus standard deviation. p Value pertains to the comparison between groups with and without ventricular arrhythmia/unexplained syncope events. SSF = spatial scale filter.

[Table 3: Log rank results.](#) Log rank, p value, optimised thresholds and number of patients within the low and high risk group are shown, as stratified according to each TA-CMR parameter. SSF = spatial scale filter.

[Table 4: ROC analysis for different predictors of outcome.](#) Detailed results of received operating characteristics curves for different predictors of outcome identified by univariable analysis. SSF = spatial scale filter. LVEF = left ventricular ejection fraction.

1

2

3

Table 1		Baseline Patient Characteristics		
Characteristic	All patients (N = 76)	Ventricular arrhythmia or unexplained syncope (n = 14)	No ventricular arrhythmia or unexplained syncope (n = 62)	p Value
Age (yrs)	61.51 ± 11.4	67.9 ± 10.0	60.1 ± 12.0	0.01
Male	66 (80%)	13 (93%)	53 (85%)	0.4
Clinical history				
Diabetes mellitus	21 (28%)	4 (29%)	17 (27%)	0.96
Hypertension	58 (76%)	11 (79%)	47 (76%)	0.78
Cigarette smoker	19 (25%)	3 (21%)	16 (26%)	0.60
Hypercholesterolemia	47 (62%)	10 (71%)	37 (60%)	0.45
Atrial fibrillation	9 (12%)	1 (7%)	8 (13%)	0.48
Prior revascularisation				
CABG	12 (16%)	3 (21%)	9 (15%)	0.61
PCI	42 (55%)	7 (50%)	35 (56%)	0.59
Cardiac MRI				
Scar burden (% of LV mass)	4.2 ± 2.4	4.9 ± 2.3	4.0 ± 2.4	0.24
LVEF (%)	51.8 (42.5-61.8)	44.5 (25.7-51.2)	54.6 (44.3-62.1)	0.01
LV EDV (ml)	175.4 (140.3-212)	202.5 (179-261.5)	170 (133.5-207.5)	0.02
LV EDV/m2	86.5 (76.3-107)	106 (90-125.3)	83 (75.3-100.3)	0.01
LV ESV (ml)	82 (56.3-119)	106.5 (82-177.5)	73.5 (51.8-114)	0.01
LV ESV/m2	39.5 (29-58.8)	55.5 (43.1-88)	35.5 (27.8-54.8)	0.01
LV mass (g)	105.7 ± 46.7	112.4 ± 54.2	103.9 ± 45.1	0.59
LV mass/m2	60.4 ± 16.4	66.9 ± 19.4	58.9 ± 15.5	0.19
RVEF (%)	58.2 (51.5-63)	57.7 (46.6-65.4)	58.5 (51.6-63)	0.74
RV EDV (ml)	148 (121.3-173)	143.5 (115.5-173.8)	150 (121.8-173.3)	0.88
RV EDV/m2	75 (61.3-87)	71 (58-97.8)	76 (62-86.3)	0.96
RV ESV (ml)	62 (46.3-81.8)	41 (42.8-89.8)	62 (47.8-79.5)	0.79
RV ESV/m2	31 (22-39.5)	31 (21-43.7)	31 (24-40)	0.81
LA (cm ²)	25.1 ± 5.8	27.6 ± 4.2	24.5 ± 5.9	0.03
RA (cm ²)	27.9 ± 44.8	23.1 ± 5.5	29.0 ± 49.6	0.36

4

5

Table 2	Texture Analysis Results			
Statistical parameters	All patients (N = 76)	Ventricular arrhythmia or unexplained syncope (n = 14)	No ventricular arrhythmia or unexplained syncope (n = 62)	p Value
SSF2				
Mean intensity	247.3 ± 169.4	244.5 ± 222.36	247.9 ± 157.4	0.960
Standard deviation	542.5 ± 280.5	430.9 ± 249.6	567.7 ± 282.8	0.085
Entropy	6.0 ± 0.6	5.9 ± 0.4	6.0 ± 0.7	0.400
Mean of positive pixels	550.4 ± 283.7	460.0 ± 285.7	570.8 ± 281.5	0.204
Skewness Maximum	0.3 ± 0.3	0.2 ± 0.3	0.3 ± 0.3	0.274
Skewness Average	0.2 ± 0.3	0.1 ± 0.2	0.2 ± 0.3	0.068
Skewness Minimum	0.1 ± 0.3	-0.1 ± 0.2	0.1 ± 0.3	0.046
Kurtosis Maximum	0.1 ± 0.6	0.2 ± 0.6	0.1 ± 0.7	0.488
Kurtosis Average	-0.1 ± 0.5	0 ± 0.3	-0.1 ± 0.5	0.762
Kurtosis Minimum	-0.3 ± 0.5	-0.3 ± 0.3	-0.3 ± 0.5	0.962
SSF3				
Mean intensity	304.5 ± 245.8	343.4 ± 301.2	295.7 ± 233.5	0.586
Standard deviation	593.9 ± 314.6	474.3 ± 299.1	621.0 ± 314.0	0.116
Entropy	6.0 ± 0.63	5.9 ± 0.4	6.0 ± 0.7	0.415
Mean of positive pixels	629.7 ± 336.2	554.2 ± 363.1	646.8 ± 330.5	0.392
Skewness _{max}	0.2 ± 0.3	0.2 ± 0.3	0.2 ± 0.3	0.754
Skewness _{avg}	0.1 ± 0.3	0.0 ± 0.3	0.1 ± 0.3	0.537
Skewness _{min}	-0.1 ± 0.4	-0.2 ± 0.4	0.0 ± 0.4	0.350
Kurtosis _{max}	0.0 ± 0.6	0.2 ± 0.7	0.0 ± 0.6	0.287
Kurtosis _{avg}	-0.2 ± 0.5	0.0 ± 0.6	-0.2 ± 0.4	0.248
Kurtosis _{min}	-0.3 ± 0.5	-0.2 ± 0.7	-0.4 ± 0.5	0.276
SSF4				
Mean intensity	306.7 ± 312.8	394.2 ± 347.8	287.0 ± 304.0	0.301
Standard deviation	606.6 ± 324.1	486.4 ± 314.7	633.8 ± 322.5	0.131
Entropy	6.0 ± 0.6	5.9 ± 0.4	6.0 ± 0.7	0.415
Mean of positive pixels	647.5 ± 360.3	601.8 ± 402.8	657.9 ± 352.7	0.636
Skewness _{max}	0.1 ± 0.4	0.2 ± 0.4	0.1 ± 0.4	0.398
Skewness _{avg}	-0.1 ± 0.3	0.0 ± 0.3	-0.1 ± 0.3	0.557
Skewness _{min}	-0.2 ± 0.4	-0.2 ± 0.4	-0.2 ± 0.3	0.994
Kurtosis _{max}	-0.1 ± 0.7	0.2 ± 0.5	-0.1 ± 0.7	0.074
Kurtosis _{avg}	-0.3 ± 0.4	-0.1 ± 0.5	-0.4 ± 0.4	0.056
Kurtosis _{min}	-0.5 ± 0.4	-0.3 ± 0.6	-0.5 ± 0.4	0.108
SSF5				
Mean intensity	279.2 ± 367.6	408.2 ± 370.3	250.0 ± 363.7	0.163
Standard deviation	609.7 ± 328.1	483.7 ± 310.0	638.2 ± 327.7	0.111
Entropy	6.0 ± 0.6	5.9 ± 0.4	6.0 ± 0.7	0.444
Mean of positive pixels	646.7 ± 373.6	613.2 ± 416.1	654.2 ± 366.6	0.737
Skewness _{max}	0.0 ± 0.4	0.1 ± 0.4	0.0 ± 0.4	0.570
Skewness _{avg}	-0.1 ± 0.3	-0.1 ± 0.3	-0.1 ± 0.3	0.732
Skewness _{min}	-0.3 ± 0.3	-0.3 ± 0.4	-0.3 ± 0.3	0.865
Kurtosis _{max}	-0.2 ± 0.5	0.0 ± 0.3	-0.3 ± 0.5	0.005
Kurtosis _{avg}	-0.4 ± 0.4	-0.2 ± 0.3	-0.5 ± 0.4	0.007
Kurtosis _{min}	-0.6 ± 0.4	-0.4 ± 0.4	-0.7 ± 0.4	0.052
SSF6				
Mean intensity	239.9 ± 409.4	398.0 ± 376.4	204.2 ± 410.9	0.102
Standard deviation	605.0 ± 332.2	476.4 ± 300.4	634.1 ± 334.3	0.097
Entropy	6.0 ± 0.6	5.9 ± 0.4	6.0 ± 0.7	0.540
Mean of positive pixels	631.7 ± 382.0	607.2 ± 417.9	637.2 ± 376.9	0.808
Skewness _{max}	0.0 ± 0.4	-0.1 ± 0.4	0.0 ± 0.4	0.713
Skewness _{avg}	-0.1 ± 0.3	-0.2 ± 0.4	-0.2 ± 0.3	0.665
Skewness _{min}	-0.3 ± 0.3	-0.4 ± 0.4	-0.3 ± 0.4	0.511
Kurtosis _{max}	-0.2 ± 0.5	-0.1 ± 0.4	-0.4 ± 0.5	0.025
Kurtosis _{avg}	-0.4 ± 0.4	-0.3 ± 0.3	-0.6 ± 0.3	0.015
Kurtosis _{min}	-0.6 ± 0.4	-0.5 ± 0.4	-0.7 ± 0.3	0.075

1

2

Table 3	Kaplan Meier Analysis				
	Log Rank	p Value	ROC Analysis Threshold	Number of patients assigned to the low risk group by TA-CMR	Number of patients assigned to the high risk group by TA-CMR
SSF2					
Skewness _{min}	4.460	0.035	0.120	25	51
SSF5					
Kurtosis _{max}	5.319	0.021	-0.445	53	23
Kurtosis _{avg}	6.397	0.011	-0.493	45	31
SSF6					
Kurtosis _{max}	8.407	0.004	-0.465	47	29
Kurtosis _{avg}	6.343	0.012	-0.628	51	25

1

2

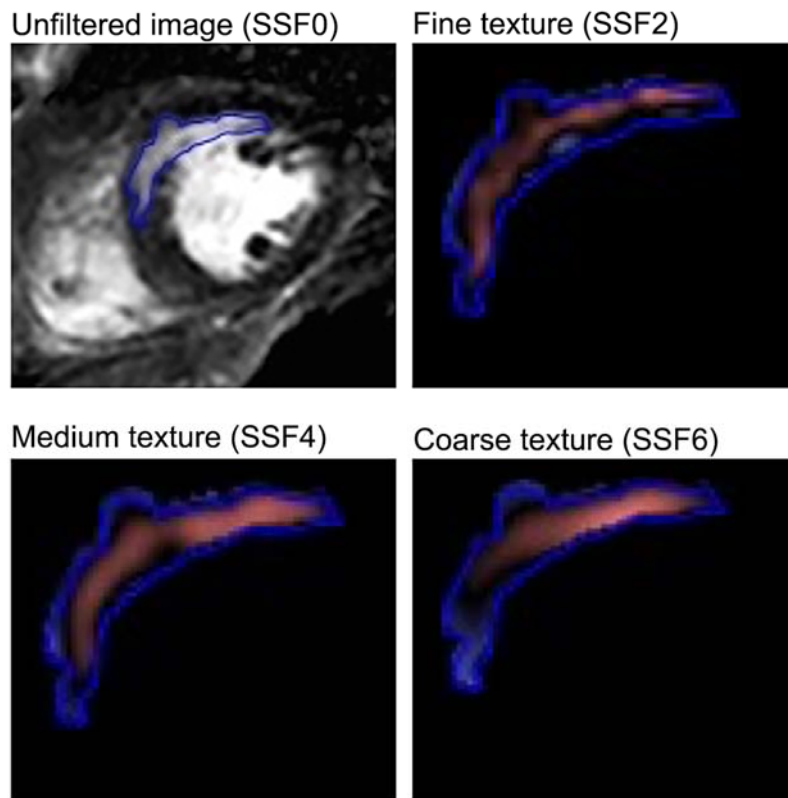
3

Table 4	Detailed results of ROC analysis for different predictors of outcome				
Test result variables	Area	SE	p-value	Asymptotic 95% confidence interval	
				Lower bound	Upper bound
Age	0.7	0.075	0.02	0.554	0.847
LVEF	0.715	0.082	0.012	0.554	0.876
Kurtosis _{avg} SSF=5	0.73	0.064	0.008	0.605	0.855
Kurtosis _{max} SSF=5	0.729	0.063	0.008	0.604	0.853
Kurtosis _{min} SSF=5	0.654	0.077	0.073	0.504	0.805
Kurtosis _{avg} SSF=6	0.715	0.066	0.012	0.586	0.845
Kurtosis _{max} SSF=6	0.705	0.063	0.017	0.582	0.828
Kurtosis _{min} SSF=6	0.656	0.079	0.07	0.5	0.811
Skewness _{avg} SSF=2	0.589	0.089	0.299	0.415	0.763
Skewness _{max} SSF=2	0.586	0.087	0.318	0.415	0.757
Skewness _{min} SSF=2	0.594	0.076	0.275	0.445	0.742

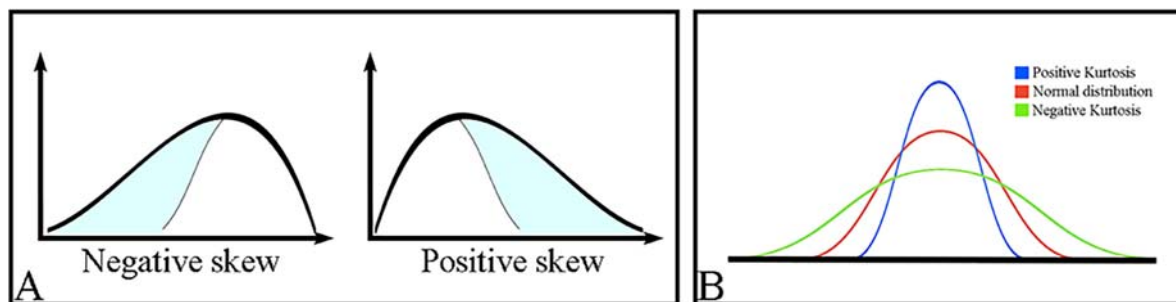
4

1 **Figures and Tables**

2 **Fig. 1**



5 **Fig. 2**

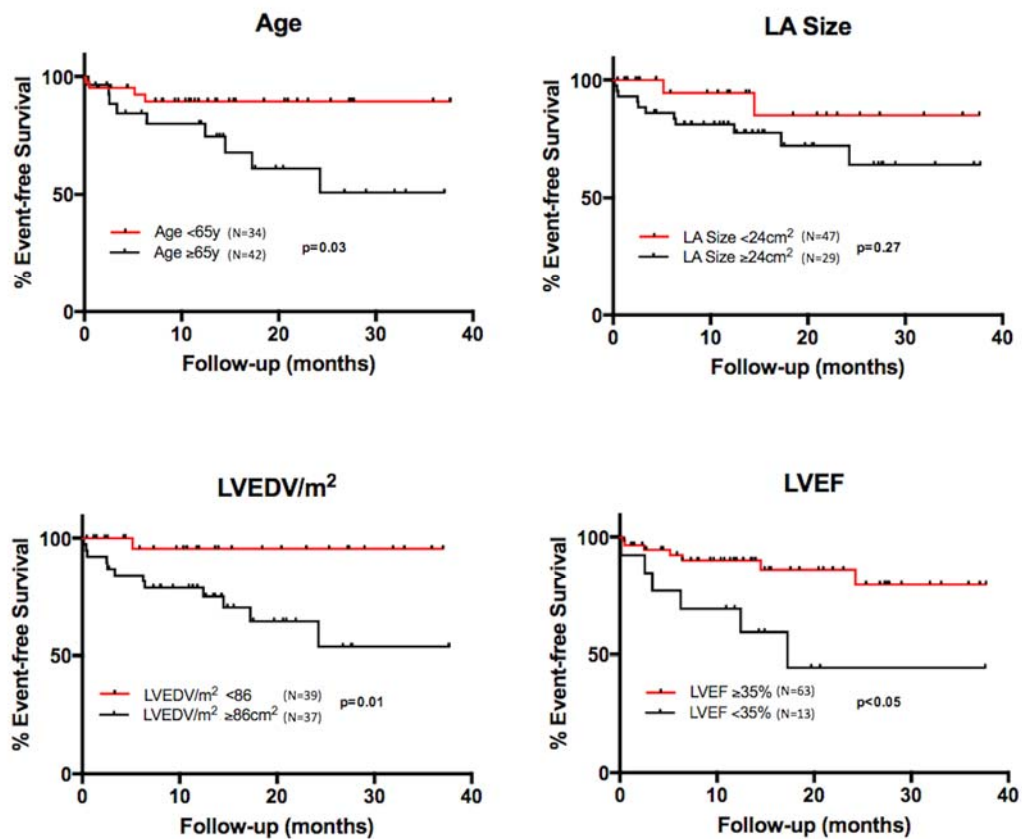


6

7

8

9 Fig. 3



10 **Fig. 4**

11

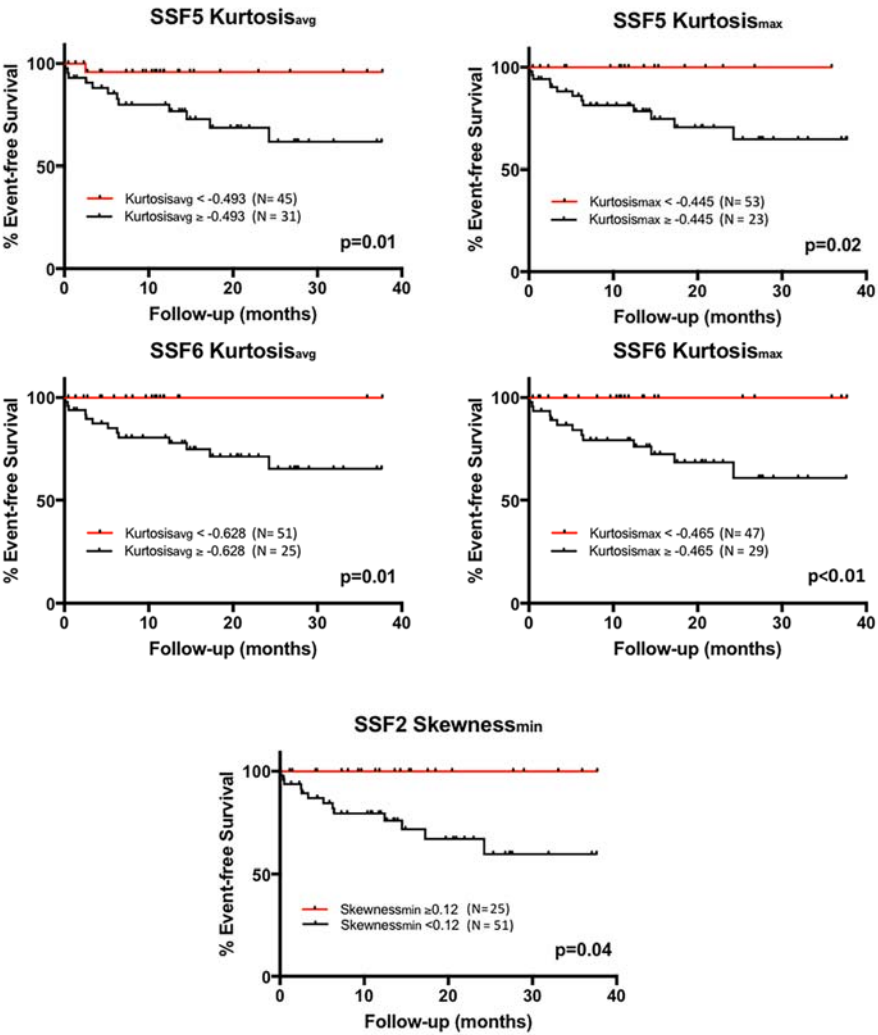


Fig. 5

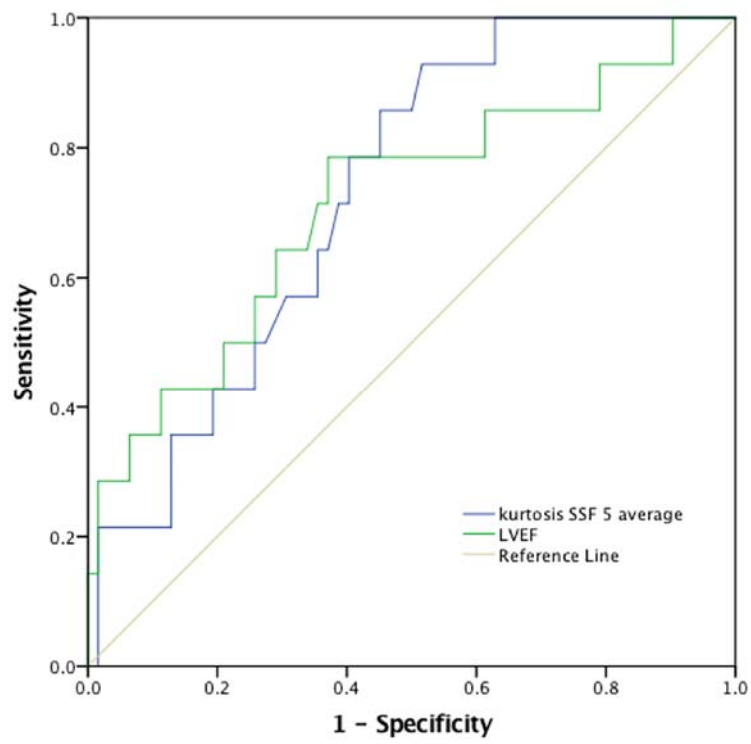


Table 1		Baseline Patient Characteristics		
Characteristic	All patients (N = 76)	Ventricular arrhythmia or unexplained syncope (n = 14)	No ventricular arrhythmia or unexplained syncope (n = 62)	p Value
Age (yrs)	61.51 ± 11.4	67.9 ± 10.0	60.1 ± 12.0	0.01
Male	66 (80%)	13 (93%)	53 (85%)	0.4
Clinical history				
Diabetes mellitus	21 (28%)	4 (29%)	17 (27%)	0.96
Hypertension	58 (76%)	11 (79%)	47 (76%)	0.78
Cigarette smoker	19 (25%)	3 (21%)	16 (26%)	0.60
Hypercholesterolemia	47 (62%)	10 (71%)	37 (60%)	0.45
Atrial fibrillation	9 (12%)	1 (7%)	8 (13%)	0.48
Prior revascularisation				
CABG	12 (16%)	3 (21%)	9 (15%)	0.61
PCI	42 (55%)	7 (50%)	35 (56%)	0.59
Cardiac MRI				
Scar burden (% of LV mass)	4.2 ± 2.4	4.9 ± 2.3	4.0 ± 2.4	0.24
LVEF (%)	51.8 (42.5-61.8)	44.5 (25.7-51.2)	54.6 (44.3-62.1)	0.01
LV EDV (ml)	175.4 (140.3-212)	202.5 (179-261.5)	170 (133.5-207.5)	0.02
LV EDV/m2	86.5 (76.3-107)	106 (90-125.3)	83 (75.3-100.3)	0.01
LV ESV (ml)	82 (56.3-119)	106.5 (82-177.5)	73.5 (51.8-114)	0.01
LV ESV/m2	39.5 (29-58.8)	55.5 (43.1-88)	35.5 (27.8-54.8)	0.01
LV mass (g)	105.7 ± 46.7	112.4 ± 54.2	103.9 ± 45.1	0.59
LV mass/m2	60.4 ± 16.4	66.9 ± 19.4	58.9 ± 15.5	0.19
RVEF (%)	58.2 (51.5-63)	57.7 (46.6-65.4)	58.5 (51.6-63)	0.74
RV EDV (ml)	148 (121.3-173)	143.5 (115.5-173.8)	150 (121.8-173.3)	0.88
RV EDV/m2	75 (61.3-87)	71 (58-97.8)	76 (62-86.3)	0.96
RV ESV (ml)	62 (46.3-81.8)	41 (42.8-89.8)	62 (47.8-79.5)	0.79
RV ESV/m2	31 (22-39.5)	31 (21-43.7)	31 (24-40)	0.81
LA (cm ²)	25.1 ± 5.8	27.6 ± 4.2	24.5 ± 5.9	0.03
RA (cm ²)	27.9 ± 44.8	23.1 ± 5.5	29.0 ± 49.6	0.36

Table 2	Texture Analysis Results			
Statistical parameters	All patients (N = 76)	Ventricular arrhythmia or unexplained syncope (n = 14)	No ventricular arrhythmia or unexplained syncope (n = 62)	p Value
SSF2				
Mean intensity	247.3 ± 169.4	244.5 ± 222.36	247.9 ± 157.4	0.960
Standard deviation	542.5 ± 280.5	430.9 ± 249.6	567.7 ± 282.8	0.085
Entropy	6.0 ± 0.6	5.9 ± 0.4	6.0 ± 0.7	0.400
Mean of positive pixels	550.4 ± 283.7	460.0 ± 285.7	570.8 ± 281.5	0.204
Skewness Maximum	0.3 ± 0.3	0.2 ± 0.3	0.3 ± 0.3	0.274
Skewness Average	0.2 ± 0.3	0.1 ± 0.2	0.2 ± 0.3	0.068
Skewness Minimum	0.1 ± 0.3	-0.1 ± 0.2	0.1 ± 0.3	0.046
Kurtosis Maximum	0.1 ± 0.6	0.2 ± 0.6	0.1 ± 0.7	0.488
Kurtosis Average	-0.1 ± 0.5	0 ± 0.3	-0.1 ± 0.5	0.762
Kurtosis Minimum	-0.3 ± 0.5	-0.3 ± 0.3	-0.3 ± 0.5	0.962
SSF3				
Mean intensity	304.5 ± 245.8	343.4 ± 301.2	295.7 ± 233.5	0.586
Standard deviation	593.9 ± 314.6	474.3 ± 299.1	621.0 ± 314.0	0.116
Entropy	6.0 ± 0.63	5.9 ± 0.4	6.0 ± 0.7	0.415
Mean of positive pixels	629.7 ± 336.2	554.2 ± 363.1	646.8 ± 330.5	0.392
Skewness _{max}	0.2 ± 0.3	0.2 ± 0.3	0.2 ± 0.3	0.754
Skewness _{avg}	0.1 ± 0.3	0.0 ± 0.3	0.1 ± 0.3	0.537
Skewness _{min}	-0.1 ± 0.4	-0.2 ± 0.4	0.0 ± 0.4	0.350
Kurtosis _{max}	0.0 ± 0.6	0.2 ± 0.7	0.0 ± 0.6	0.287
Kurtosis _{avg}	-0.2 ± 0.5	0.0 ± 0.6	-0.2 ± 0.4	0.248
Kurtosis _{min}	-0.3 ± 0.5	-0.2 ± 0.7	-0.4 ± 0.5	0.276
SSF4				
Mean intensity	306.7 ± 312.8	394.2 ± 347.8	287.0 ± 304.0	0.301
Standard deviation	606.6 ± 324.1	486.4 ± 314.7	633.8 ± 322.5	0.131
Entropy	6.0 ± 0.6	5.9 ± 0.4	6.0 ± 0.7	0.415
Mean of positive pixels	647.5 ± 360.3	601.8 ± 402.8	657.9 ± 352.7	0.636
Skewness _{max}	0.1 ± 0.4	0.2 ± 0.4	0.1 ± 0.4	0.398
Skewness _{avg}	-0.1 ± 0.3	0.0 ± 0.3	-0.1 ± 0.3	0.557
Skewness _{min}	-0.2 ± 0.4	-0.2 ± 0.4	-0.2 ± 0.3	0.994
Kurtosis _{max}	-0.1 ± 0.7	0.2 ± 0.5	-0.1 ± 0.7	0.074
Kurtosis _{avg}	-0.3 ± 0.4	-0.1 ± 0.5	-0.4 ± 0.4	0.056
Kurtosis _{min}	-0.5 ± 0.4	-0.3 ± 0.6	-0.5 ± 0.4	0.108
SSF5				
Mean intensity	279.2 ± 367.6	408.2 ± 370.3	250.0 ± 363.7	0.163
Standard deviation	609.7 ± 328.1	483.7 ± 310.0	638.2 ± 327.7	0.111
Entropy	6.0 ± 0.6	5.9 ± 0.4	6.0 ± 0.7	0.444
Mean of positive pixels	646.7 ± 373.6	613.2 ± 416.1	654.2 ± 366.6	0.737
Skewness _{max}	0.0 ± 0.4	0.1 ± 0.4	0.0 ± 0.4	0.570
Skewness _{avg}	-0.1 ± 0.3	-0.1 ± 0.3	-0.1 ± 0.3	0.732
Skewness _{min}	-0.3 ± 0.3	-0.3 ± 0.4	-0.3 ± 0.3	0.865
Kurtosis _{max}	-0.2 ± 0.5	0.0 ± 0.3	-0.3 ± 0.5	0.005
Kurtosis _{avg}	-0.4 ± 0.4	-0.2 ± 0.3	-0.5 ± 0.4	0.007
Kurtosis _{min}	-0.6 ± 0.4	-0.4 ± 0.4	-0.7 ± 0.4	0.052
SSF6				
Mean intensity	239.9 ± 409.4	398.0 ± 376.4	204.2 ± 410.9	0.102
Standard deviation	605.0 ± 332.2	476.4 ± 300.4	634.1 ± 334.3	0.097
Entropy	6.0 ± 0.6	5.9 ± 0.4	6.0 ± 0.7	0.540
Mean of positive pixels	631.7 ± 382.0	607.2 ± 417.9	637.2 ± 376.9	0.808
Skewness _{max}	0.0 ± 0.4	-0.1 ± 0.4	0.0 ± 0.4	0.713
Skewness _{avg}	-0.1 ± 0.3	-0.2 ± 0.4	-0.2 ± 0.3	0.665
Skewness _{min}	-0.3 ± 0.3	-0.4 ± 0.4	-0.3 ± 0.4	0.511
Kurtosis _{max}	-0.2 ± 0.5	-0.1 ± 0.4	-0.4 ± 0.5	0.025
Kurtosis _{avg}	-0.4 ± 0.4	-0.3 ± 0.3	-0.6 ± 0.3	0.015
Kurtosis _{min}	-0.6 ± 0.4	-0.5 ± 0.4	-0.7 ± 0.3	0.075

29

30

31

32

33

Table 3	Kaplan Meier Analysis				
	Log Rank	p Value	ROC Analysis Threshold	Number of patients assigned to the low risk group by TA-CMR	Number of patients assigned to the high risk group by TA-CMR
SSF2					
Skewness _{min}	4.460	0.035	0.120	25	51
SSF5					
Kurtosis _{max}	5.319	0.021	-0.445	53	23
Kurtosis _{avg}	6.397	0.011	-0.493	45	31
SSF6					
Kurtosis _{max}	8.407	0.004	-0.465	47	29
Kurtosis _{avg}	6.343	0.012	-0.628	51	25

34

35

36

37

38

Table 4		Detailed results of ROC analysis for different predictors of outcome			
Test result variables	Area	SE	p-value	Asymptotic 95% confidence interval	
				Lower bound	Upper bound
Age	0.7	0.075	0.02	0.554	0.847
LVEF	0.715	0.082	0.012	0.554	0.876
Kurtosis _{avg} SSF=5	0.73	0.064	0.008	0.605	0.855
Kurtosis _{max} SSF=5	0.729	0.063	0.008	0.604	0.853
Kurtosis _{min} SSF=5	0.654	0.077	0.073	0.504	0.805
Kurtosis _{avg} SSF=6	0.715	0.066	0.012	0.586	0.845
Kurtosis _{max} SSF=6	0.705	0.063	0.017	0.582	0.828
Kurtosis _{min} SSF=6	0.656	0.079	0.07	0.5	0.811
Skewness _{avg} SSF=2	0.589	0.089	0.299	0.415	0.763
Skewness _{max} SSF=2	0.586	0.087	0.318	0.415	0.757
Skewness _{min} SSF=2	0.594	0.076	0.275	0.445	0.742

39

40

41

